International Journal of
*Environmental Research and Public Health*

MDPI

*Article*

# Influence of Humic Acids on the Removal of Arsenic and Antimony by Potassium Ferrate

**Ning Wang [1,2,*], Wenwen Li [1], Nannan Wang [3], Man Li [4] and Hongbo Wang [1,2]**

[1] School of Municipal and Environmental Engineering, Shandong Jianzhu University, Jinan 250101, China
[2] Resources and Environment Innovation Institute, Shandong Jianzhu University, Jinan 250101, China
[3] Qingdao Municipal Engineering Design and Research Institute, Qingdao 266061, China
[4] Shandong Soil Pollution Prevention and Recalcination Center, Jinan 250033, China
* Correspondence: wangning@sdjzu.edu.cn

**Abstract:** Although the removal ability of potassium ferrate ($K_2FeO_4$) on aqueous heavy metals has been confirmed by many researchers, little information focuses on the difference between the individual and simultaneous treatment of elements from the same family of the periodic table. In this project, two heavy metals, arsenic (As) and antimony (Sb) were chosen as the target pollutants to investigate the removal ability of $K_2FeO_4$ and the influence of humic acid (HA) in simulated water and spiked lake water samples. The results showed that the removal efficiencies of both pollutants gradually increased along the Fe/As or Sb mass ratios. The maximum removal rate of As(III) reached 99.5% at a pH of 5.6 and a Fe/As mass ratio of 4.6 when the initial As(III) concentration was 0.5 mg/L; while the maximum was 99.61% for Sb(III) at a pH of 4.5 and Fe/Sb of 22.6 when the initial Sb(III) concentration was 0.5 mg/L. It was found that HA inhibited the removal of individual As or Sb slightly and the removal efficiency of Sb was significantly higher than that of As with or without the addition of $K_2FeO_4$. For the co-existence system of As and Sb, the removal of As was improved sharply after the addition of $K_2FeO_4$, higher than Sb; while the latter was slightly better than that of As without $K_2FeO_4$, probably due to the stronger complexing ability of HA and Sb. X-ray energy dispersive spectroscopy (EDS), X-ray diffractometer (XRD), and X-ray photoelectron spectroscopy (XPS) were used to characterize the precipitated products to reveal the potential removal mechanisms based on the experimental results.

**Keywords:** potassium ferrate; As(III); Sb(III); mass ratio; humic acid (HA)

check for updates

**Citation:** Wang, N.; Li, W.; Wang, N.; Li, M.; Wang, H. Influence of Humic Acids on the Removal of Arsenic and Antimony by Potassium Ferrate. *Int. J. Environ. Res. Public Health* **2023**, *20*, 4317. https://doi.org/10.3390/ijerph20054317

Academic Editor: Hui Yin

Received: 25 January 2023
Revised: 16 February 2023
Accepted: 18 February 2023
Published: 28 February 2023

**Copyright:** © 2023 by the authors. Licensee MDPI, Basel, Switzerland. This article is an open access article distributed under the terms and conditions of the Creative Commons Attribution (CC BY) license (https://creativecommons.org/licenses/by/4.0/).

## 1. Introduction

Given that by 2025, two-thirds of the world's population will experience severe water shortages, securing water usage is one of the crucial concerns for researchers in the 21st century [1]. Heavy metals in the water environment harm aquatic ecosystems [2] and accumulate in food chains causing damage to the liver, the heart, and the nervous system of humans [3]. Arsenic and antimony are two carcinogenic heavy metals that have received significant attention from scientists and researchers [4]. Approximately 188,000 tons of antimony was consumed globally in 2016, about five times as much as arsenic [5]. In recent years, arsenic and antimony pollution incidents have occurred more frequently in major environmental matrices [6,7].

It has been reported that arsenic is naturally present in 31 groundwaters in various nations and areas in Asia, Europe, and the Americas [6]. This groundwater is used by millions of people for drinking and agriculture, thus endangering their health [6]. Artificial arsenic sources include mining, arsenic-containing pesticides, herbicides, and crop desiccants, as well as other processes such as industrial wastewater discharge and chemical waste treatment [8]. Chronic poisoning can occur when a person is exposed to excessive levels of arsenic for an extended period of time, causing the element to accumulate in the skin, hair,

and nails [9]. Arsenic primarily exists in the form of arsenate ($AsO_4^{3-}$) and nitrite ($AsO_3^{3-}$) in natural water bodies. $H_2AsO_4^-$ and $HAsO_4^{2-}$ dominate the aqueous solutions at a pH value of 4–8; while, $H_3AsO_3$ outnumbers other species when the pH is less than 9 under reducing conditions [10]. As(III) is approximately 60 times as toxic as $A_S$(V). Previous studies have shown that many thousands of tons of aromatic arsenic compounds are used in veterinary drugs and in feed additives in poultry and swine farms, and released into the environment via solid waste and wastewater discharging [11]. Although the compounds are not highly toxic, they can transform into carcinogenic and highly mobile inorganics containing As(III) and As(V) and threaten the biosafety of the ecosystem [12–14].

Sb mostly has two valence states, being Sb(III) and Sb(V), similar to As, in environmental, biological, and geochemical contexts. Antimony exists in the form of $Sb(OH)^{6-}$ under oxidation conditions, and $Sb(OH)_3$, $Sb(OH)^{2+}$ and $Sb(OH)^{4-}$ under reducing conditions [15]. Antimony is commonly used in the production of batteries, flame retardants, fabrics, plastics, ammunition, ceramic emulsifiers, and glass decolorants [16], of which approximately 60% is utilized as flame retardants and 20% as alloys [17]. Antimony may cause nausea, vomiting, and diarrhea even with very brief exposure, and it is considered carcinogenic over a longer time frame [18]. Sb(III) is reported to be 10 times more hazardous than Sb(V) [19,20], similar to As(III).

Flocculation is a common technique among various practices for controlling aqueous arsenic and antimony. Guo et al. [21] presented that 98% Sb(V) could be removed by 130 mg/L of ferric chloride flocculant at properly pH value, while As(V) needed only 5 mg/L to achieve the same removal rate. Adsorption is another popular option. Chammui et al. [22] made inexpensive activated carbon from coal mine waste residue to remove As(III) and As(V) from water. However, the adsorption method has restrictions being the low treatment efficiency and treatment of spend adsorbent. Some biological methods, such as sulfate-reducing bacteria (SBR) could reduce Sb(V) into Sb (III) and deposit Sb (III) with excessive sulfide in the form of $Sb_2S_3$ [23]. The lengthy microbial culture cycle and toxic inhibition, however, limit the application of this approach. Additionally, since arsenic and antimony are frequently observed co-existing in natural environments [24,25], it is necessary to develop simultaneous elimination techniques. Ferrate has been used in multi-metal ions removal processes. For instance, Liu et al. [26] reported that the combined effect of Fe(VI) and Mn(II) resulted in the adsorption of TI(I) and $TI(OH)_3$ by the negatively charged ferric (hydro)oxides/$MnO_2$ flocs, achieving the effective removal of trace TI from polluted waters. Song et al. [27] utilized electrolysis to remove both metal elements and found that the highest removal efficiency of arsenic and antimony was 98.69% and 94.45%, respectively, when the electrode distance was 2 cm. Other researchers have attempted to use inexpensive iron-based compounds to extract arsenic and antimony from wastewater. For instance, Sekula et al. [28] constructed an on-site treatment system for arsenic and antimony removal from neutral mine drainage water with zero-valent iron, producing high levels of removal rates (89% for As and 84% for Sb). According to Shan et al. [29], magnetic nanoparticles coated with hematite were effective at removing both As and Sb. This implies that iron-based materials have the potential for the concurrent removal of arsenic and antimony from wastewater. Lan et al. [30] reported a synergistic impact of DP/Ferrate on the simultaneous adsorption of As and Sb.

Natural organic matters (NOMs) exist in most natural waters and most of them are highly sensitive to iron oxides [31]. Additionally, the existence of these dissolved organics would also react with/influence many target pollutants during the treatment by ferrate, such as iodide and total iodine [32], bisphenol A & F, acetaminophen, and 4-tert-butylphenol [33]. Previous studies have demonstrated that NOMs directly impact on the transformation of iron minerals [34]. One significant category of NOMs is humic acid (HA), which influences the removal process of aqueous heavy metals. HA tends to be adsorbed on various mineral colloids, which affects the transport of mineral colloids and the pollutants they adsorbed [35]. It has been reported that a high concentration of HA prevents or delays the transition of Fe(III) in a mineral phase with low crystallization [31,36].

Since the HA concentrations (0–100 mg/L) are many orders of magnitude higher in natural waters than those of heavy metals, this may have a major effect on the formation and surface binding of the ions [37]. Therefore, it is crucial to investigate how HA affects the removal of As and Sb by $K_2FeO_4$. In this project, $K_2FeO_4$ was employed to remove aqueous As(III) and Sb(III), and various influencing factors were investigated, including iron-antimony/-arsenic mass ratio and humic acid (HA). Additionally, the experiments were conducted and compared between in spiked surface water and synthetic water samples.

## 2. Materials and Methods

### 2.1. Reagents and Solutions

100 mg/L arsenic and antimony standard stock solution was prepared in our laboratory and the configuration was as following: (1) 0.1320 g of $As_2O_3$ (analytical grade, Sinopharm Chemical Reagent Co., Ltd., Beijing, China) was dried at 105 °C for 2 h and dissolved in 5 mL of 1 M NaOH (analytical grade, Sinopharm Chemical Reagent Co., Ltd. Beijing, China) in solution. Then 1 M HCl (excellent grade pure, Sinopharm Chemical Reagent Co., Ltd. Beijing, China) was used to neutralize the solution until the red color of phenolphthalein (analytical grade, Tianjin Damao Chemical Reagent Factory, Tianjin, China) faded, and the solution was transferred and diluted in a 1000 mL volumetric flask before being stored in a brown glass bottle at 4 °C; (2) 0.1197 g of $Sb_2O_3$ (analytical grade, Shanghai Yien Chemical Technology Co., Ltd., Shanghai, China) was weighed to prepare stock solution mostly following the previous procedure, except using 80 mL concentrated HCl to dissolve the solid instead of NaOH solution and adding another 120 mL concentrated HCl in the 1000 mL volumetric flask. The $K_2FeO_4$ used in this experiment came from a laboratory of Zhejiang University (purity > 95%), which was synthesized using the method of Thompson et al. [38]. The $K_2FeO_4$ were made by the hypochlorite method using concentrated sodium hypochlorite solution oxidize hydrous ferric oxide, whose precursor was ferric nitrate. Chromite titration [39] was used to check the purity prior of each test. The HA was purchased from Tianjin Guangfu Fine Chemical Research Institute, Tianjin, China (HA Commercial ID: CP500G).

### 2.2. Experiments for Aqueous Heavy Metal Removal

A series of 300 mL simulated water samples (As/Sb dissolved in deionized water) containing certain amounts of As(III)/Sb(III) individually or both were used to carry out the removal experiments by potassium ferrate at room temperature using different dosage mass ratios with HA present or absent. A six-paddle programmable jar tester was set to a quick stir at 250 r/min for 3 min, a slow stir at 60 r/min for 20 min, and then a settlement for 30 min. An amount of supernatant was sampled and filtered using a 0.45 μm microporous filter membrane before being transferred into a colorimetric tube for additional instrument analysis. The remaining As and Sb concentrations in the supernatant was determined using an atomic fluorescence photometer (AFS-933, Beijing Jitian Instrument Co., Ltd., Beijing, China). All glassware used in the process had been soaked in a 10% nitric acid solution for at least 24 h, rinsed with tap water, washed at least three times with deionized water, and dried before usage.

Raw water samples from Yingxue Lake at Shandong Jianzhu University were selected for actual surface water experiments. The characteristics of the water quality were tested and listed in Table S1. The concentrations of As and Sb were 2.55 μg/L and 4.39 μg/L in the raw water, respectively. Therefore, the surface water samples were spiked to adjust both values to 0.5 mg/L in order to prevent increasing comparison test error brought on by low concentrations of the target contaminants.

### 2.3. Surface Characterization

The separated precipitates from the aforementioned experiments were freeze-dried with a freeze dryer (SCIENTZ-10N, Ningbo Xinzhi Biotechnology Co., Ltd., Ningbo, China)

for 24 h for surface characterization with X-ray energy spectrometer (EDS, ESCALAB 250Xi, Thermo Fisher Scientific Co., Ltd., Waltham, MA, USA), X-ray diffractometer (XRD, smart lab 3 kw, RIGAKU Co., Ltd., Tokyo, Japan), and X-ray photoelectron spectrometer (XPS, Escalab 250Xi, Thermo Fisher Scientific Ltd., Waltham, MA, USA). EDS was used to characterize the appearance and element content of the solid samples. The precipitate was magnified 10,000 times or 12,000 times. More details can be found in the previous publication [40]. XRD could identify the surface crystalline phase properties. The precipitates were characterized by a diffractometer at 40 kV and 30 mA. The scanning range was 10~90°, with an interval of 0.02°. For XPS, the sample was compressed into 1 cm × 1 cm pellets and a full-spectrum analysis was performed with a monochromatic Alka excitation source (HV = 1486.6 eV, power = 150 W, beam diameter = 400 μm, and C1s were calibrated as 284.8 eV).

## 3. Results and Discussion

### *3.1. The Effect of Mass Ratio on the Removal Effect of Arsenic and Antimony*

The effects of Fe/As mass ratios (Fe/As) on As removal rate were investigated, when the initial As(III) concentration was 0.5 mg/L. As can be seen in Figure 1a, the removal efficiency of As increased rapidly as the Fe/As increased until it reached a steady state. The maximum value of 99.55% occurred at Fe/As = 4.6, and the dosage of $K_2FeO_4$ (measured by Fe) of 2.3 mg/L. At this time, the remaining As concentration was less than 0.05 mg/L, which satisfied the requirements of TypeI~III water of the Environmental Quality Standard for Surface Water (GB3838-2002). The removal rate of As increased from 8.58% (Fe/As = 1.1) initially to 97.24% (Fe/As = 3.4), and then gradually increased to 100% (Fe/As = 6.8) with the continuous increase of Fe/As until stabilizing. In the beginning, the ratio of Fe/As was low, resulting in an insufficient amount of $K_2FeO_4$ and with fewer opportunities for contact with As. More $K_2FeO_4$ significantly improved the removal rate of As, as the ratio increased. The results could support the significant effect of $K_2FeO_4$ on the removal of As. It has been reported that the primary mechanism of elimination by $K_2FeO_4$ is the oxidation of As(III) to the less toxic and more easily removable As(V) [41]. The reduced form, $Fe(OH)_3$, serves as a potential adsorbent [42]. The reaction equations are presented as follows (Equations (1) and (2)) [40].

$$2HFeO_4^- + 3H_3AsO_3 \rightarrow 2Fe^{3+} + H_3AsO_4^{2-} \quad (1)$$

$$Fe^{3+} + 3H_2O \rightarrow Fe(OH)_3 + 3H^+ \quad (2)$$

$$AsO_4^{3-} + Fe^{3+} = FeAsO_4 \downarrow \quad (3)$$

In addition, Fe(III) also reacted with As(V), which was formed after oxidation, and finally produced iron arsenate ($FeAsO_4$) precipitate (Equation (3)). This provides another way for As(III) to be removed. The formed particles showed a large number of lamellar structures, around 30 nm (Figure S1a). It was possibly a dual mechanism resulting in irregular morphology, unlike the spherical particle flocs produced by $K_2FeO_4$ removing Sb (Figure S2a). However, since $FeAsO_4$ gradually disappeared under neutral and alkaline conditions [43], As was mostly removed by $K_2FeO_4$ by adsorption.

Figure S1b presents the EDS spectrum of the precipitates formed when $K_2FeO_4$ reacted with aqueous As. It was evident that O, Cl, K, Fe, and As were the most prevalent elements in the deposits. The presence of As confirmed the elimination process carried out by $K_2FeO_4$. In addition, the XRD spectrum demonstrated that the characteristic diffraction peaks at 2θ of 22.15°, 26.71° and 28.77° were the characteristic diffraction peaks of $FeAsO_4$ (JCPDS No. 78-1545). This implies that the mechanism of As removed by $K_2FeO_4$ could be attributed to the reduction of Fe(VI) into Fe(III) and the subsequent reaction precipitating $FeAsO_4$ between Fe(III) and As(V). Additionally, the characteristic diffraction peak of $Fe_3(AsO_4)_2$ at 2θ of 40.91° suggested that As was removed by the oxidation of $K_2FeO_4$ to form $Fe_3(AsO_4)_2$ in Figure S1c [44].

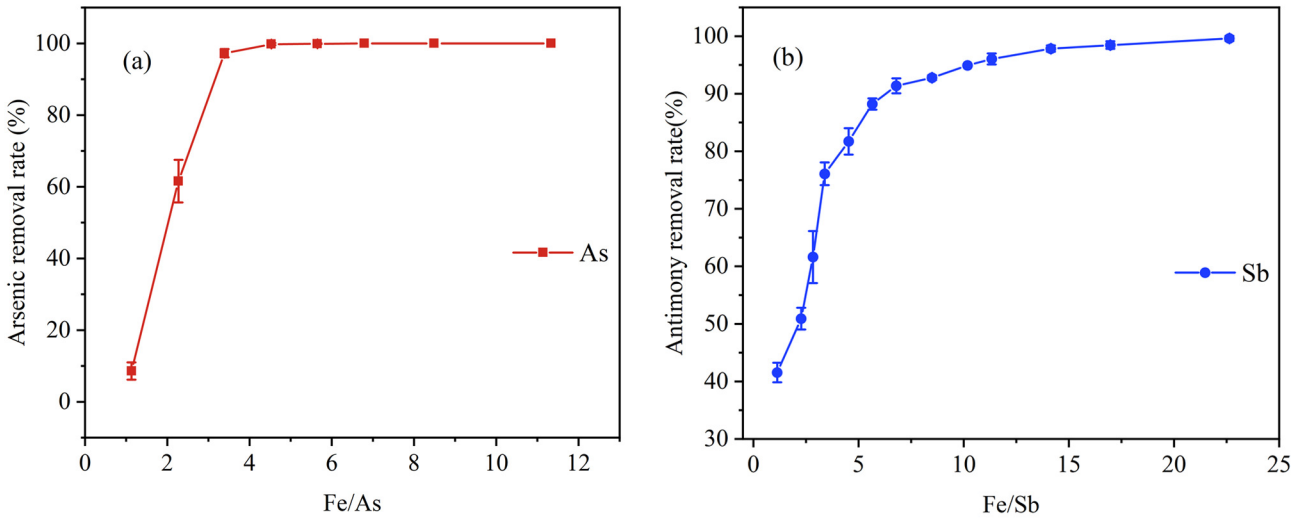



**Figure 1.** (**a**) Effect of Fe/As mass ratio on removal of individual arsenic, initial As(III) = 0.5 mg/L pH = 6.5 (**b**) Effect of Fe/Sb mass ratio on removal of individual antimony, initial Sb(III) = 0.5 mg/L pH = 4.5.

Additionally, Figure 2c shows the characteristic diffraction peaks of $Fe(OH)_3$ (2θ of 41.15°) and FeO(OH) (2θ of 40.89°), indicating that the reduction process of $K_2FeO_4$ might generate ferrous-containing colloid particles with adsorption potential. The flocculation caused by $K_2FeO_4$ is attributed to the single charged $Fe(OH)_3$ colloid as well as a complex form of iron (hydrogen) oxide compound [45]. Some researchers have already found that the hydrolysis product of $K_2FeO_4$ is a 2-linear ferrihydrite with the smallest crystalline form of iron (hydrogen)oxide [46]. Ferrihydrite has a relatively high surface area and a large number of binding sites for complexing with heavy metals. T Adsorption, specifically the occurrence of a surface complexation event, may be the primary determinant of As removal [30]. The XPS full-scan spectrum (Figure S1d) also showed that Fe, O, K, C, and As were the main elements in the precipitates, consistent with the conclusions from the EDS spectrum (Figure S1b).

As shown in Figure 1b, the profile was similar to As, gradually increasing at the beginning until stabilizing at the initial Sb(III) concentration of 0.5 mg/L. The removal efficiency of Sb was sharply improved to more than 90% as the ratio increased to 6.8. When Fe/Sb was 22.6, namely the dosage of $K_2FeO_4$ (calculated as Fe) of 11.31 mg/L, the removal rate reached 99.61%, while the remaining Sb in the solution was less than 0.005 mg/L, meeting the requirements of the "Surface Water Centralized Drinking Water Sources" (GB 3838-2002) and the "Emission Standards for Tin, Antimony and Mercury Industrial Pollutants" (GB 30770-2014). The pH of 4.5 was chosen with reference to the previous study of Wang et al. [40]. When the pH values were between 4 and 5, $K_2FeO_4$ showed better and more constant removal of Sb with a removal efficiency close to 70%. Since the initial concentration of Sb was constant, more K2FeO4 was dosed as the ratio of Fe/Sb increased. A greater amount of $Fe(OH)_3$ was also produced by the reduction of $K_2FeO_4$ in the solution, resulting in a more intense adsorption effect on the Sb ions. In Figure S2c, the diffraction peaks of $Sb_2O_5$ were found at 2θ of 28.77°, 75.66° and 84.38°, suggesting the oxidation of Sb(III) to Sb(V) by $K_2FeO_4$. Clearly, the removal consumed a greater amount of $K_2FeO_4$. Sb(V), formed by oxidation by $K_2FeO_4$, was reportedly less ready to be adsorbed than As(V) [40]. It may be due to the fact that the ionic radius of Sb is larger than that of As [47], requiring more adsorbent to attach, and the amount of $K_2FeO_4$ added in the process of removing Sb is larger than As. Based on these XPS plots (Figures S1d and S2d) and previous research [40], the binding energies of 45.6 eV and 530.1 eV are assigned to As 3d [48] and Sb 3d [49], respectively, indicating the formation of As (V) and Sb (V) on the surface of the $K_2FeO_4$ hydrolysate. Additionally, the higher content of Cl and Na

elements were also found in the EDS plot (Figure S2b), possibly due to the addition of excessive HCl to inhibit the hydrolysis of antimony ions during the preparation of the stock solution, and the addition of NaOH to neutralize it in the later process of the pH adjustment. Meanwhile, the stronger diffraction peaks at 2θ of 32.12°, 45.86° and 56.85° in the XRD pattern (Figure S2c) were the characteristic diffraction peaks of NaCl (JCPDS No. 88-2300), which was consistent with the results of the EDS pattern.

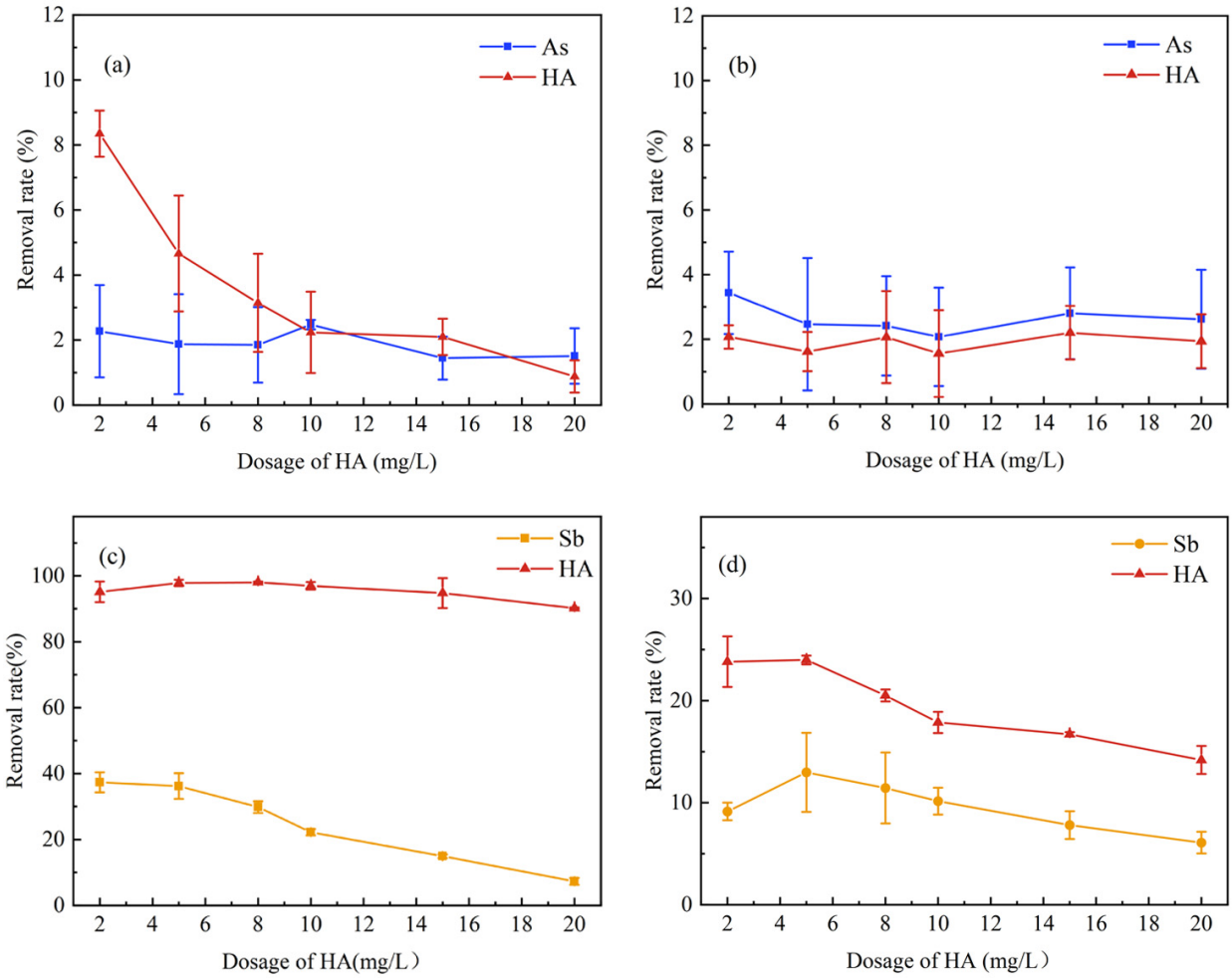



**Figure 2.** Effect of HA concentration on the removal of As and Sb ((**a**) $K_2FeO_4$(Fe of 2.26 mg/L) +HA + As, pH = 6.5; (**b**) HA + As, pH = 6.5; (**c**) $K_2FeO_4$ (Fe of 3.39 mg/L) + HA + Sb, pH = 4.5; (**d**) HA + Sb, pH = 4.5).

### *3.2. The Effect of Humic Acid on the Removal of Aqueous Antimony and Arsenic*

Figure 2a,b showed the impact of HA on $K_2FeO_4$ removing As. It could be seen that compared with zero dosage, the addition of $K_2FeO_4$ had no significant effect on the removal rate of As, which was less than 4% for both circumstances. It could be attributed to the insufficient dosing of $K_2FeO_4$, which was mostly consumed by the HA first. As shown in Figure 2a,b the lower concentrations of HA were more influenced by $K_2FeO_4$. HA contains a series of negatively charged macromolecules, possibly altering the surface charge and the transport retention characteristics of iron mineral colloids [50,51]. As a result, the colloids may develop a negatively-charged surface and consume some adsorption sites, inhibiting As adhering to the ferrite minerals. In addition, the higher anion binding sites in HA may precipitate with cationic iron at an appropriate dose of $K_2FeO_4$ to form an insoluble complex due to the charge neutralization [52], which facilitates the removal of HA. Therefore, the dosage of $K_2FeO_4$ is generally sufficient under the condition of a low

concentration of HA, which could be removed to a certain extent in the solution. As the HA concentration increased, the removal rate gradually decreased possibly due to the depletion of $K_2FeO_4$. Overall, the interaction between HA and $K_2FeO_4$ can inhibit the removal of As.

The influence of HA on the removal of Sb could be seen in Figure 2c,d. Similar to the elimination of As, the presence of HA also inhibited the removal process of $K_2FeO_4$ on Sb, since the removal efficiency gradually declined with the HA concentration. This could possibly be attributed to hydrophobic HA molecules competing for the active sites by forming stable complexes on the surface of the precipitates containing iron. However, the removal rates were much higher for Sb and HA than those found in the experiments for As, as can be seen by comparing Figure 2a,c. It is unclear whether the combination between Sb and HA would facilitate the removal of both substances with $K_2FeO_4$. The higher removal rate could be explained by the fact that the core of the Sb(III) molecule has stronger cationic characteristics than As(III), resulting in a better combination with HA through complexation [53] and mutually promoting the removal for both. Therefore, both rates were also higher than As in the control group without any iron mineral (Figure 2d). A further explanation may be that HA has the potential to strongly alter the distribution of Sb (particle, colloid, and dissolved portion) and to change the redox morphology of Sb (Sb(V) relative to Sb(III) abundance), when Sb was initially combined with iron (Fe(III)) oxides such as hydrophyte [54]. In Figure 2d, HA had a certain removal effect on Sb(III) in the absence of $K_2FeO_4$, owing to carboxyl, phenolic and amine groups present in HA complexing with Sb(III) through a ligand exchange reaction of the Sb(III) center under acidic conditions [55].

Figure 3a illustrates the effect of the dosage of HA on the simultaneous removal of As and Sb by $K_2FeO_4$. Both HA and As were mostly eliminated while the removal rate of Sb was relatively lower (The highest removal rate was only 18.27%). The removal efficiencies of As and Sb both showed a gradual descent with the increase of HA concentration. Dissolved organic matter may occupy the active sites of the absorbent, thus inhibiting the adsorption of the target pollutants in natural waters [56,57]. Therefore, in-situ reduced ferric particles from $K_2FeO_4$ reduction may be encapsulated by HA, subsequently negatively affecting the removal of As and Sb. In Figure 3b, HA also showed certain removal effects on As and Sb without adding $K_2FeO_4$.

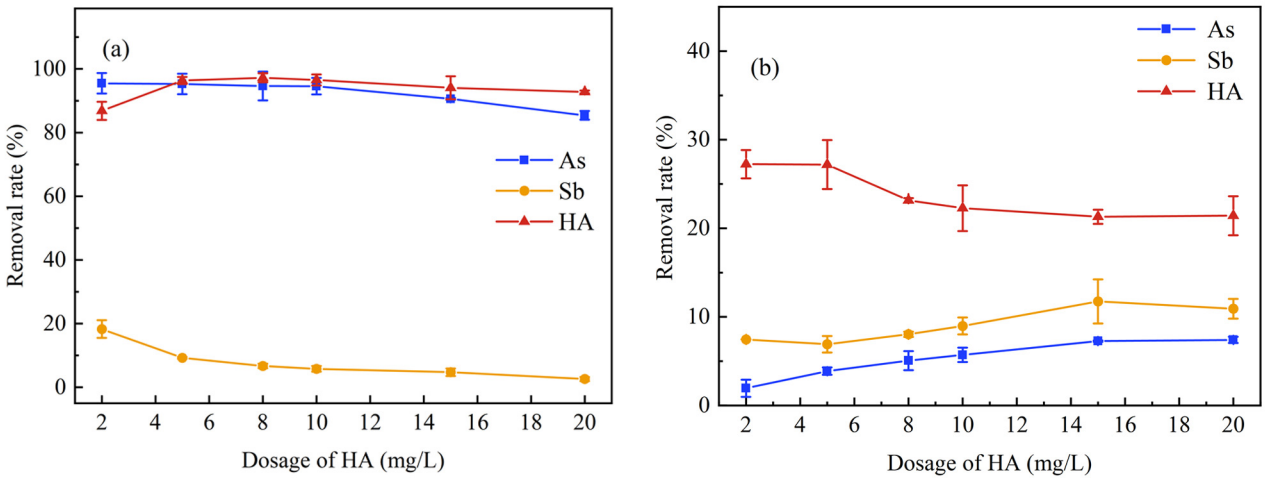



**Figure 3.** Effect of HA dosing on the simultaneous removal of As and Sb. (**a**) $K_2FeO_4$ (Fe of 8.48 mg/L) treatment; (**b**) no $K_2FeO_4$.

Therefore, $K_2FeO_4$ could improve the removal of As and HA as can be seen by comparing Figure 3a,b. According to Figure 4a, it can be seen that the simultaneous removal experiments enhanced the removal of As significantly. Additionally, the dose of $K_2FeO_4$ in the solution was excessive to remove As and Sb simultaneously at low HA concentration, which made it easier to eliminate both As and HA. As was more readily removed than

Sb, resulting in a higher efficiency during the simultaneous removal. In Figure 4b, Sb was more easily separated than As during either the individual or simultaneous treatments without $K_2FeO_4$ added. This result may be due to the superior complexing ability of HA and Sb. Previous studies have proposed two mechanisms for HA to complex with Sb(III): (1) Ligand exchange at the center of Sb and release of one or two hydroxides respectively; (2) Formation of negatively charged complexes. In addition, chelation, H-bridge, or cationic metal can stabilize Sb(III) bound to humic acid [55].

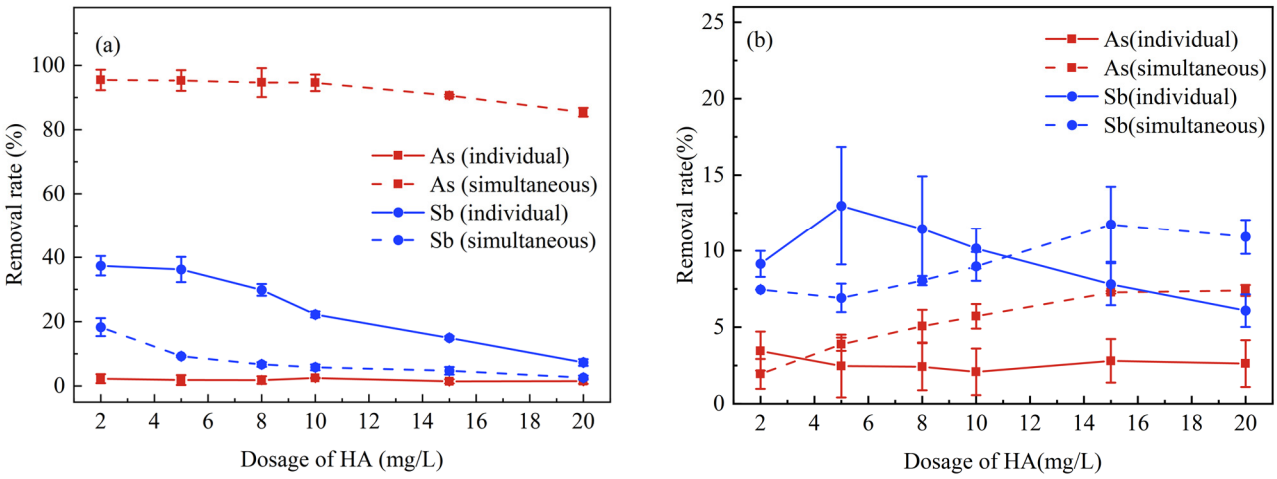



**Figure 4.** Comparison of HA dosing on the removal of As(III) and Sb(III) between individual and simultaneous treatments ((**a**) $K_2FeO_4$ treatment; (**b**) no $K_2FeO_4$).

### *3.3. The Removal of Arsenic and Antimony by Potassium Ferrate in Surface Water and Simulated Water Samples*

The results shown in Figure 5 present the comparison of the removal between the spiked actual surface water and the simulated water. It was found that the removal rates and patterns of As were comparable between the spiked actual water and the simulated water. The removal rate in the simulated water was slightly higher than that in the actual water samples and both curves rose sharply between 1–4 mg/L of $K_2FeO_4$ and. Almost 100% of the heavy metals were removed from both kinds of water samples (Figure 5a) after $K_2FeO_4$ concentration increased to a certain threshold. This indicated that the effect of other pollutants in the actual water body on the removal of As by $K_2FeO_4$ was minimal and essentially negligible.

However, the removal of Sb was substantially lower in the spiked actual water bodies. The removal rate of Sb in the simulated water increased to 40% when the concentration of $K_2FeO_4$ was increased to 2 mg/L, while 10 mg/L $K_2FeO_4$ was needed for the spiked actual water to reach the equivalent effect (Figure 5b). This phenomenon may be caused by the fact that the presence of other pollutants in the spiked actual water body affected the removal of Sb rather than As. It has been reported that a competitive relationship between Sb and N exists, because of the competition between Sb and N in order to occupy the group-V positions [42]. In addition, Ma et al. [58] found that Sb and atomic-N compete for the same positions under atomic-N-rich conditions. These [42] adversely affect the adsorption efficiency of Sb at the adsorption sites on iron nanoparticles and weaken the removal of Sb.

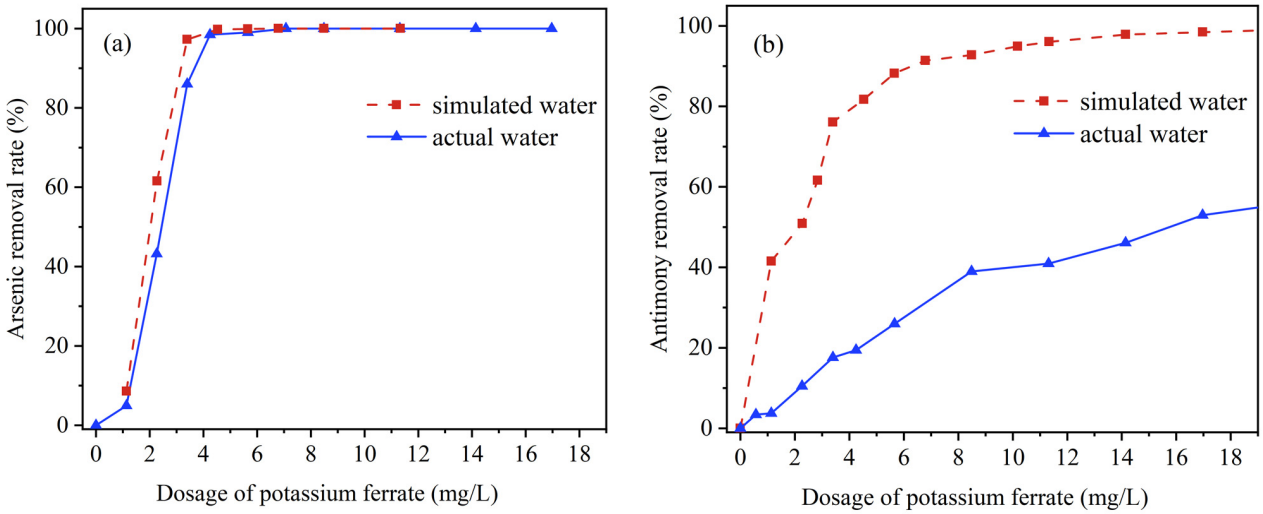



**Figure 5.** Dosage of $K_2FeO_4$ effect on actual water and simulate water ((**a**) arsenic removal by $K_2FeO_4$, (**b**) antimony removal by $K_2FeO_4$).

## 4. Conclusions

The removal of As(III) and Sb(III) by $K_2FeO_4$ was influenced by the Fe/metal mass ratio and HA. The removal rates rose with the ratios and the maximums for As and Sb occurred, respectively, at Fe/As = 4.6 and Fe/Sb = 6.8. The removal rates increased as a function of the ratios. The HA in water could inhibit the removal of As and Sb, mainly because HA formed the colloid with the negatively-charged surface or competed for adsorption sites on the ferrite minerals. In the binary system, the removal performance of As was improved, while Sb was slightly easier to remove if there was no $K_2FeO_4$, possibly due to the strong complexation between HA and Sb. It was found that the removal impact of As was not significantly different in the spiked actual surface water and the simulated water, while it was significantly different for Sb. It is speculated that the substances in the spiked actual water competed for the flocculation of potassium ferrate hydrolysates, which was intended to remove Sb.

**Supplementary Materials:** The following supporting information can be downloaded at: https://www.mdpi.com/article/10.3390/ijerph20054317/s1, Figure S1: Surface characterization of the precipitation products of individual As removal by 6 K2FeO4 (a: SEM, 10,000 times, b: EDS, c: XRD, d: XPS); Figure S2: Surface characterization of the precipitation products of individual Sb removal by 9 K2FeO4 (a: SEM, 12,000 times, b: EDS, c: XRD, d: XPS); Table S1: Water quality parameters of Yingxue Lake (five samples).

**Author Contributions:** W.L., N.W. (Nannan Wang) and M.L., data curation; N.W. (Ning Wang) and H.W., funding acquisition; H.W., supervision; N.W. (Ning Wang) and W.L., writing—original draft; N.W. (Ning Wang), writing—review & editing. All authors have read and agreed to the published version of the manuscript.

**Funding:** This work was supported by the Shandong Provincial Natural Science Foundation (Grant no. ZR2020ME228); Shandong Major Scientific and Technological Innovation Project (Grant no. 2022CXGC021001) and the Introduction and Cultivation Plan for Young Innovative Talents of Colleges and Universities.

**Institutional Review Board Statement:** Not applicable.

**Informed Consent Statement:** Not applicable.

**Data Availability Statement:** Not applicable.

**Conflicts of Interest:** The authors declare no conflict of interest.

## References


1. Schwarzenbach, R.P.; Egli, T.; Hofstetter, T.B.; von Gunten, U.; Wehrli, B. Global Water Pollution and Human Health. *Annu. Rev. Environ. Resour.* **2010**, *35*, 109–136. [CrossRef]
2. Green, A.J.; Planchart, A. The neurological toxicity of heavy metals: A fish perspective. *Comp. Biochem. Physiol. Part C Toxicol. Pharmacol.* **2018**, *208*, 12–19. [CrossRef]
3. Gall, J.E.; Boyd, R.S.; Rajakaruna, N. Transfer of heavy metals through terrestrial food webs: A review. *Environ. Monit. Assess.* **2015**, *187*, 201. [CrossRef]
4. Sun, X.; Li, B.; Han, F.; Xiao, E.; Xiao, T.; Sun, W. Impacts of Arsenic and Antimony Co-Contamination on Sedimentary Microbial Communities in Rivers with Different Pollution Gradients. *Microb. Ecol.* **2019**, *78*, 589–602. [CrossRef] [PubMed]
5. Wu, D.; Sun, S.P.; He, M.; Wu, Z.; Xiao, J.; Chen, X.D.; Wu, W.D. As(V) and Sb(V) co-adsorption onto ferrihydrite: Synergistic effect of Sb(V) on As(V) under competitive conditions. *Environ. Sci. Pollut. Res. Int.* **2018**, *25*, 14585–14594. [CrossRef]
6. Shahid, M.; Niazi, N.K.; Dumat, C.; Naidu, R.; Khalid, S.; Rahman, M.M.; Bibi, I. A meta-analysis of the distribution, sources and health risks of arsenic-contaminated groundwater in Pakistan. *Environ. Pollut.* **2018**, *242*, 307–319. [CrossRef]
7. Ungureanu, G.; Filote, C.; Santos, S.C.R.; Boaventura, R.A.R.; Volf, I.; Botelho, C.M.S. Antimony oxyanions uptake by green marine macroalgae. *J. Environ. Chem. Eng.* **2016**, *4*, 3441–3450. [CrossRef]
8. Bang, S.; Korfiatis, G.P.; Meng, X. Removal of arsenic from water by zero-valent iron. *J. Hazard. Mater.* **2005**, *121*, 61–67. [CrossRef]
9. Chen, Y.; Parvez, F.; Gamble, M.; Islam, T.; Ahmed, A.; Argos, M.; Graziano, J.H.; Ahsan, H. Arsenic exposure at low-to-moderate levels and skin lesions, arsenic metabolism, neurological functions, and biomarkers for respiratory and cardiovascular diseases: Review of recent findings from the Health Effects of Arsenic Longitudinal Study (HEALS) in Bangladesh. *Toxicol. Appl. Pharmacol.* **2009**, *239*, 184–192. [CrossRef]
10. Ungureanu, G.; Santos, S.; Boaventura, R.; Botelho, C. Arsenic and antimony in water and wastewater: Overview of removal techniques with special reference to latest advances in adsorption. *J. Environ. Manag.* **2015**, *151*, 326–342. [CrossRef]
11. Hu, Y.; Zhang, W.; Cheng, H.; Tao, S. Public Health Risk of Arsenic Species in Chicken Tissues from Live Poultry Markets of Guangdong Province, China. *Environ. Sci. Technol.* **2017**, *51*, 3508–3517. [CrossRef] [PubMed]
12. Cortinas, I.; Field, J.A.; Kopplin, M.; Garbarino, J.R.; Gandolfi, A.J.; Sierra-Alvarez, R. Anaerobic Biotransformation of Roxarsone and Related N-Substituted Phenylarsonic Acids. *Environ. Sci. Technol.* **2006**, *40*, 2951–2957. [CrossRef] [PubMed]
13. Yang, T.; Wang, L.; Liu, Y.; Jiang, J.; Huang, Z.; Pang, S.Y.; Cheng, H.; Gao, D.; Ma, J. Removal of Organoarsenic with Ferrate and Ferrate Resultant Nanoparticles: Oxidation and Adsorption. *Environ. Sci. Technol.* **2018**, *52*, 13325–13335. [CrossRef] [PubMed]
14. Yang, T.; Liu, Y.; Wang, L.; Jiang, J.; Huang, Z.; Pang, S.-Y.; Cheng, H.; Gao, D.; Ma, J. Highly effective oxidation of roxarsone by ferrate and simultaneous arsenic removal with in situ formed ferric nanoparticles. *Water Res.* **2018**, *147*, 321–330. [CrossRef] [PubMed]
15. Wang, L.; Wan, C.L.; Zhang, Y.; Lee, D.J.; Liu, X.; Chen, X.F.; Tay, J.H. Mechanism of enhanced Sb(V) removal from aqueous solution using chemically modified aerobic granules. *J. Hazard. Mater.* **2015**, *284*, 43–49. [CrossRef]
16. Rakshit, S.; Sarkar, D.; Punamiya, P.; Datta, R. Antimony sorption at gibbsite-water interface. *Chemosphere* **2011**, *84*, 480–483. [CrossRef] [PubMed]
17. Biswas, B.K.; Inoue, J.; Kawakita, H.; Ohto, K.; Inoue, K. Effective removal and recovery of antimony using metal-loaded saponified orange waste. *J. Hazard. Mater.* **2009**, *172*, 721–728. [CrossRef]
18. Mantha, Z.; Mitrakas, M.; Tzollas, N.; Stylianou, S.; Katsoyiannis, I.; Zouboulis, A. Removal of Antimony Species, Sb(III)/Sb(V), from Water by Using Iron Coagulants. *Water* **2018**, *10*, 1328. [CrossRef]
19. Krachler, M.; Emons, H. Speciation of antimony for the 21st century: Promises and pitfalls. *Trends Anal. Chem.* **2001**, *20*, 79–90. [CrossRef]
20. Smichowski, P.; Madrid, Y.; Cámara, C. Analytical methods for antimony speciation in waters attrace and ultratrace levels. A review. *Fresenius J. Anal. Chem.* **1998**, *360*, 623–629. [CrossRef]
21. Guo, X.; Wu, Z.; He, M. Removal of antimony(V) and antimony(III) from drinking water by coagulation-flocculation-sedimentation (CFS). *Water Res.* **2009**, *43*, 4327–4335. [CrossRef] [PubMed]
22. Chammui, Y.; Sooksamiti, P.; Naksata, W.; Thiansem, S.; Arqueropanyo, O.-A. Removal of arsenic from aqueous solution by adsorption on Leonardite. *Chem. Eng. J.* **2014**, *240*, 202–210. [CrossRef]
23. Wang, H.; Chen, F.; Mu, S.; Zhang, D.; Pan, X.; Lee, D.J.; Chang, J.S. Removal of antimony (Sb(V)) from Sb mine drainage: Biological sulfate reduction and sulfide oxidation-precipitation. *Bioresour. Technol.* **2013**, *146*, 799–802. [CrossRef] [PubMed]
24. Sun, W.; Xiao, E.; Dong, Y.; Tang, S.; Krumins, V.; Ning, Z.; Sun, M.; Zhao, Y.; Wu, S.; Xiao, T. Profiling microbial community in a watershed heavily contaminated by an active antimony (Sb) mine in Southwest China. *Sci. Total Environ.* **2016**, *550*, 297–308. [CrossRef] [PubMed]
25. Hiller, E.; Lalinská, B.; Chovan, M.; Jurkovič, Ľ.; Klimko, T.; Jankulár, M.; Hovorič, R.; Šottník, P.; Fľaková, R.; Ženišová, Z.; et al. Arsenic and antimony contamination of waters, stream sediments and soils in the vicinity of abandoned antimony mines in the Western Carpathians, Slovakia. *Appl. Geochem.* **2012**, *27*, 598–614. [CrossRef]
26. Liu, Y.-L.; Li, Y.-T.; Wang, L.; Wang, W.; Ma, J. Enhanced Trace Tl Removal with Ferrate through the Addition of Mn(II): Effect and Mechanism. *ACS EST Eng.* **2021**, *1*, 571–580. [CrossRef]

27. Song, P.; Song, Q.; Yang, Z.; Zeng, G.; Xu, H.; Li, X.; Xiong, W. Numerical simulation and exploration of electrocoagulation process for arsenic and antimony removal: Electric field, flow field, and mass transfer studies. *J. Environ. Manag.* **2018**, *228*, 336–345. [CrossRef]
28. Sekula, P.; Hiller, E.; Šottník, P.; Jurkovič, L'.; Klimko, T.; Vozár, J. Removal of antimony and arsenic from circum-neutral mine drainage in Poproč, Slovakia: A field treatment system using low-cost iron-based material. *Environ. Earth Sci.* **2018**, *77*, 518. [CrossRef]
29. Shan, C.; Ma, Z.; Tong, M. Efficient removal of trace antimony(III) through adsorption by hematite modified magnetic nanoparticles. *J. Hazard. Mater.* **2014**, *268*, 229–236. [CrossRef]
30. Lan, B.; Wang, Y.; Wang, X.; Zhou, X.; Kang, Y.; Li, L. Aqueous arsenic (As) and antimony (Sb) removal by potassium ferrate. *Chem. Eng. J.* **2016**, *292*, 389–397. [CrossRef]
31. Chen, C.; Kukkadapu, R.; Sparks, D.L. Influence of Coprecipitated Organic Matter on Fe2+(aq)-Catalyzed Transformation of Ferrihydrite: Implications for Carbon Dynamics. *Environ. Sci. Technol.* **2015**, *49*, 10927–10936. [CrossRef]
32. Wang, X.-S.; Liu, Y.-L.; Li, M.; Song, H.; Huang, X.; Gao, Z.; Zhang, J.; Cui, C.-W.; Liu, B.-C.; Ma, J.; et al. Occurrence of Iodophenols in Aquatic Environments and the Deiodination of Organic Iodine with Ferrate(VI). *Environ. Sci. Technol.* **2022**, *56*, 16104–16114. [CrossRef]
33. Zhao, X.-N.; Huang, Z.-S.; Wang, G.-J.; Liu, Y.-L.; Song, W.-W.; Ma, J.; Wang, L. Highly Efficient Utilization of Ferrate(VI) Oxidation Capacity Initiated by Mn(II) for Contaminant Oxidation: Role of Manganese Species. *Environ. Sci. Technol.* **2023**, *57*, 2527–2537. [CrossRef]
34. ThomasArrigo, L.K.; Mikutta, C.; Byrne, J.; Kappler, A.; Kretzschmar, R. Iron(II)-Catalyzed Iron Atom Exchange and Mineralogical Changes in Iron-rich Organic Freshwater Flocs: An Iron Isotope Tracer Study. *Environ. Sci. Technol.* **2017**, *51*, 6897–6907. [CrossRef]
35. Weng; van Riemsdijk, W.H.; Luuk, K.; Tjisse, H. Adsorption of Humic Substances on Goethite: Comparison between Humic Acids and Fulvic Acids. *Environ. Sci. Technol.* **2006**, *40*, 7494–7500. [CrossRef] [PubMed]
36. Jones, A.M.; Collins, R.N.; Rose, J.; Waite, T.D. The effect of silica and natural organic matter on the Fe(II)-catalysed transformation and reactivity of Fe(III) minerals. *Geochim. Cosmochim. Acta* **2009**, *73*, 4409–4422. [CrossRef]
37. Zhou, P.; Yan, H.; Gu, B. Competitive complexation of metal ions with humic substances. *Chemosphere* **2005**, *58*, 1327–1337. [CrossRef] [PubMed]
38. Thompson, G.W.; Ockbrman, L.T.; Schreyer, J.M. Preparation and Purification of Potassium Ferrate. VI. *Am. Chem. Soc.* **1951**, *73*, 1183–1185. [CrossRef]
39. Schreyer, J.M.; Thompson, G.W.; Ockerman, L.T. Oxidation of Chromium(III) with Potassium Ferrate(VI). *Anal. Chem.* **1950**, *22*, 1426–1427. [CrossRef]
40. Wang, N.; Wang, N.; Tan, L.; Zhang, R.; Zhao, Q.; Wang, H. Removal of aqueous As(III) Sb(III) by potassium ferrate ($K_2FeO_4$): The function of oxidation and flocculation. *Sci. Total Environ.* **2020**, *726*, 138541. [CrossRef] [PubMed]
41. Lee, Y.; Um, I.-h.; Yoon, J. Arsenic(III) Oxidation by Iron(VI) (Ferrate) and Subsequent Removal of Arsenic(V) by Iron(III) Coagulation. *Environ. Sci. Technol.* **2004**, *37*, 5750–5756. [CrossRef] [PubMed]
42. Braza, V.; Reyes, D.F.; Gonzalo, A.; Utrilla, A.D.; Ben, T.; Ulloa, J.M.; Gonzalez, D. Sb and N Incorporation Interplay in GaAsSbN/GaAs Epilayers near Lattice-Matching Condition for 1.0–1.16-eV Photonic Applications. *Nanoscale Res. Lett.* **2017**, *12*, 356. [CrossRef] [PubMed]
43. Jia, Y.; Xu, L.; Wang, X.; Demopoulos, G.P. Infrared spectroscopic and X-ray diffraction characterization of the nature of adsorbed arsenate on ferrihydrite. *Geochim. Cosmochim. Acta* **2007**, *71*, 1643–1654. [CrossRef]
44. Inam, M.A.; Khan, R.; Park, D.R.; Ali, B.A.; Uddin, A.; Yeom, I.T. Influence of pH and Contaminant Redox Form on the Competitive Removal of Arsenic and Antimony from Aqueous Media by Coagulation. *Minerals* **2018**, *8*, 574. [CrossRef]
45. Wang, Y.; Wang, N.; Li, M.; Bai, M.; Wang, H. Potassium ferrate enhances ozone treatment of pharmaceutical wastewaters: Oxidation and catalysis. *J. Water Process Eng.* **2022**, *49*, 103055. [CrossRef]
46. Jambor, J.L.; Dutrizac, J.E. Occurrence and Constitution of Natural and Synthetic Ferrihydrite, a Widespread Iron Oxyhydroxide. *Cheminform* **1998**, *98*, 2549–2586. [CrossRef]
47. Wu, T.L.; Cui, X.D.; Cui, P.X.; Ata-Ul-Karim, S.T.; Sun, Q.; Liu, C.; Fan, T.T.; Gong, H.; Zhou, D.M.; Wang, Y.J. Speciation and location of arsenic and antimony in rice samples around antimony mining area. *Environ. Pollut.* **2019**, *252*, 1439–1447. [CrossRef]
48. Wang, X.; Qin, X.; Wang, W.; Liu, Y.; Shi, X.; Sun, Y.; Liu, C.; Zhao, J.; Zhang, G.; Liu, H.; et al. Interface chemistry and surface morphology evolution study for InAs/Al2O3 stacks upon in situ ultrahigh vacuum annealing. *Appl. Surf. Sci.* **2018**, *443*, 567–574. [CrossRef]
49. Shi, X.; Wang, X.; Sun, Y.; Liu, C.; Wang, W.; Cheng, Y.; Wang, W.; Wang, J.; Cho, K.; Lu, F.; et al. Interface chemistry study of InSb/Al2O3 stacks upon in situ post deposition annealing by synchrotron radiation photoemission spectroscopy. *Appl. Surf. Sci.* **2017**, *425*, 932–940. [CrossRef]
50. Chen, G.; Liu, X.; Su, C. Distinct Effects of Humic Acid on Transport and Retention of $TiO_2$ Rutile Nanoparticles in Saturated Sand Columns. *Environ. Sci. Technol.* **2012**, *46*, 7142–7150. [CrossRef]
51. Wang, D.; Zhang, W.; Zhou, D. Antagonistic Effects of Humic Acid and Iron Oxyhydroxide Grain-Coating on Biochar Nanoparticle Transport in Saturated Sand. *Environ. Sci. Technol.* **2013**, *47*, 5154–5161. [CrossRef] [PubMed]
52. Sharp, E.L.; Parson, S.A.; Jefferson, B. Coagulation of NOM: Linking character to treatment. *Water Sci. Technol.* **2006**, *53*, 67–76. [CrossRef] [PubMed]

53. Buschmann, J.; Kappeler, A.; Lindauer, U.; Kistler, D.; Berg, M.; Sigg, L. Arsenite and Arsenate Binding to Dissolved Humic Acids: Influence of pH, Type of Humic Acid, and Aluminum. *Environ. Sci. Technol.* **2006**, *40*, 6015–6020. [CrossRef] [PubMed]
54. Karimian, N.; Burton, E.D.; Johnston, S.G.; Hockmann, K.; Choppala, G. Humic acid impacts antimony partitioning and speciation during iron(II)-induced ferrihydrite transformation. *Sci. Total Environ.* **2019**, *683*, 399–410. [CrossRef]
55. Buschmann, J.; Sigg, L. Antimony(III) Binding to Humic Substances: Influence of pH and Type of Humic Acid. *Environ. Sci. Technol.* **2004**, *38*, 4535–4541. [CrossRef]
56. Liu, Y.; Wang, L.; Wang, X.; Huang, Z.; Xu, C.; Yang, T.; Zhao, X.; Qi, J.; Ma, J. Highly efficient removal of trace thallium from contaminated source waters with ferrate: Role of in situ formed ferric nanoparticle. *Water Res.* **2017**, *124*, 149–157. [CrossRef]
57. Liu, Y.; Yang, T.; Wang, L.; Huang, Z.; Li, J.; Cheng, H.; Jiang, J.; Pang, S.; Qi, J.; Ma, J. Interpreting the effects of natural organic matter on antimicrobial activity of Ag(2)S nanoparticles with soft particle theory. *Water Res.* **2018**, *145*, 12–20. [CrossRef]
58. Ma, T.-C.; Lin, Y.-T.; Lin, H.-H. Effects of plasma species on the N incorporation of GaAsSbN grown by plasma-assisted gas-source molecular-beam epitaxy. *J. Cryst. Growth* **2011**, *318*, 363–366. [CrossRef]


**Disclaimer/Publisher's Note:** The statements, opinions and data contained in all publications are solely those of the individual author(s) and contributor(s) and not of MDPI and/or the editor(s). MDPI and/or the editor(s) disclaim responsibility for any injury to people or property resulting from any ideas, methods, instructions or products referred to in the content.